ISSN 0965-5425, Computational Mathematics and Mathematical Physics, 2016, Vol. 56, No. 12, pp. 2068–2078. © Pleiades Publishing, Ltd., 2016.
Original Russian Text © D.V. Sadin, 2016, published in Zhurnal Vychislitel'noi Matematiki i Matematicheskoi Fiziki, 2016, Vol. 56, No. 12, pp. 2098–2109.

TVD Scheme for Stiff Problems of Wave Dynamics of Heterogeneous Media of Nonhyperbolic Nonconservative Type

D. V. Sadin*

Mozhaisky Military Space Academy, St. Petersburg, 197198 Russia

*e-mail: *sadin@yandex.ru, vka@mil.ru*

Received October 6, 2014; in final form, May 12, 2016

Abstract—A finite-difference TVD scheme is presented for problems in nonequilibrium wave dynamics of heterogeneous media with different velocities and temperatures but with identical pressures of the phases. A nonlinear form of artificial viscosity depending on the phase relaxation time is proposed. The computed solutions are compared with exact self-similar ones for an equilibrium heterogeneous medium. The performance of the scheme is demonstrated by numerical simulation with varying particle diameters, grid sizes, and particle concentrations. It is shown that the scheme is efficient in terms of Fletcher's criterion as applied to stiff problems.

Keywords: TVD scheme, dynamics of heterogeneous media, stiff problem.

DOI: 10.1134/S0965542516120137

1. INTRODUCTION

A continual description of the wave dynamics of nonequilibrium heterogeneous media is based on equations of motion for the phase components with different velocities and temperatures, but with identical pressures [1] and also on models in which each phase has its own pressure, temperature, and velocity (see [2–5]). In the latter case, the system of equations is hyperbolic and, in the general case, nonconservative. High-order accurate shock-capturing solutions can be produced by applying, for example, modifications of Godunov's method [3], the Harten TVD scheme [4], etc. The nonconservative of equations in the solution of the Riemann problem in a nonequilibrium heterogeneous medium was addressed in [6, 7].

A feature of numerical simulation of nonequilibrium wave dynamics of heterogeneous media with identical phase pressures is that the equations of motion are not hyperbolic (see [1]). As a result, the difference schemes of [3, 4] cannot be applied, because the components of characteristics have imaginary parts. TVD schemes that do not require the hyperbolicity of the equations of motion were proposed as applied to geophysical fluid dynamics [8] with reconstruction of functions [9]. A TVD scheme for simulating the dynamics of a mixture of reactive gases and inert particles was proposed in [10]; in that scheme, the interphase interactions in the time approximation were computed at the lower time level.

There is also a class of stiff problems with widely different characteristic phase relaxation times [11–14]. In this case, a severe restriction is imposed on the Courant number (admissible time step), and the computation of interphase interactions [10, 15] at the lower time level can be not efficient. To overcome this stiffness difficulty, in the case of two-velocity and two- or three-temperature media, first-order accurate difference schemes [12, 16] and a second-order accurate TVD scheme [17] have been implemented, in which the admissible Courant number can be increased by one order of magnitude or more.

The goal of this paper is to construct a difference scheme that provides a high resolution for shock, contact, and combined discontinuities in heterogeneous nonequilibrium wave flows with identical phase pressures and applies to stiff problems with dominated convection (of hyperbolic and nonhyperbolic types).

2. WAVE DYNAMICS EQUATIONS FOR A HETEROGENEOUS MEDIUM WITH DIFFERENT PHASE VELOCITIES AND TEMPERATURES AND IDENTICAL PHASE PRESSURES

The dynamics of a heterogeneous medium with different phase velocities and temperatures and identical phase pressures is described using the Euler approach. Within the framework of a continual descrip-

tion under well-known assumptions without allowance for added mass forces, the system of equations can be written in the following equivalent form (see [1]):

$$\begin{gathered}\frac{\partial \rho_i}{\partial t}+\nabla\cdot(\rho_i\mathbf{v}_i)=0,\quad \frac{\partial}{\partial t}(\rho_1\mathbf{v}_1)+\nabla(\rho_1\mathbf{v}_1\mathbf{v}_1)+\alpha_1\nabla p=-\mathbf{F}_\mu,\\ \frac{\partial}{\partial t}(\rho_2\mathbf{v}_2)+\nabla(\rho_2\mathbf{v}_2\mathbf{v}_2)+\alpha_2\nabla p=\mathbf{F}_\mu,\quad \frac{\partial}{\partial t}(\rho_2 e_2)+\nabla\cdot(\rho_2 e_2\mathbf{v}_2)=Q,\\ \frac{\partial}{\partial t}(\rho_1E_1+\rho_2K_2)+\nabla\cdot(\rho_1E_1\mathbf{v}_1+\rho_2K_2\mathbf{v}_2)+\nabla\cdot[p(\alpha_1\mathbf{v}_1+\alpha_2\mathbf{v}_2)]=-Q,\end{gathered}\tag{2.1}$$

$$\rho_i=\rho_i^\circ\alpha_i,\quad i=1,\ 2,\quad \alpha_1+\alpha_2=1,\quad E_1=e_1+v_1^2/2,\quad K_2=v_2^2/2,\quad E_2=K_2+e_2.$$

Here and below, the subscripts 1 and 2 denote the parameters of the gas and the particles, respectively; the superscript ° denotes the true densities; ∇ is the Hamiltonian operator; α_i, ρ_i, $\mathbf{v}_i$, E_i, and e_i denote the volume fraction, reduced density, velocity, and total and internal energies per unit mass of the ith phase; p is the gas pressure; $\mathbf{F}_\mu$ is the viscous component of the phase interaction force; Q is the intensity of heat transfer between the gas and the particles in a unit volume; and t is time.

Closure relations. System (2.1) is closed by applying the equations of state of an ideal calorically perfect gas and incompressible solid particles:

$$p=(\gamma_1-1)\rho_1^\circ e_1,\quad e_1=c_vT_1,\quad e_2=c_2T_2,\quad \{\gamma_1,c_v,c_2,\rho_2^\circ\}\equiv\text{const}.$$

Here, T_1 and T_2 are the temperatures of the gas and the particles, respectively; γ_1 is the ratio of specific heats of the gas; c_v is the specific heat capacity of the gas at constant volume; and c_2 is the specific heat capacity of the particles.

The intensities of interphase friction and heat transfer, $\mathbf{F}_\mu$ and Q, are specified using well-known empirical criteria relations previously tested for the class of problems under consideration [1, 18, 19].

3. DIFFERENCE SCHEME

3.1. TVD Condition for a Stiff Scalar Transport Equation with a Source

The approach proposed is illustrated by considering the Hopf equation with a source term, which is a model gas dynamics equation with friction and heat transfer on the phase boundary [12]. Following Harten [20], we prove a sufficient condition for diminishing the total variation of the numerical solution to the Cauchy problem

$$\frac{\partial u}{\partial t}+\frac{\partial f(u)}{\partial x}=-bu,\quad a(u)=\frac{df}{du},\quad b>0,\quad u(x,0)=\phi(x),\quad -\infty<x<+\infty.$$

In the domain of the problem, we introduce a uniform Euler grid with a spatial step h and specify time levels t^k with a step τ. Consider an arbitrary one-parameter difference scheme of the form

$$u_n^{k+1}=u_n^k+C^+_{n+1/2}\Delta_{n+1/2}u^k-C^-_{n-1/2}\Delta_{n-1/2}u^k-b\tau\left[\nu u_n^{k+1}+(1-\nu)u_n^k\right],\tag{3.1}$$

where $0\le\nu\le1$ is a parameter of the scheme, $\Delta_{n+1/2}u=u_{n+1}-u_n$, n is the spatial index, and k is the time level index.

Proposition. *Let the coefficients $C^\pm$ and the time step τ in* (3.1) *satisfy the inequalities*

$$\begin{gathered}C^+_{n+1/2}\ge0,\quad C^-_{n+1/2}\ge0,\\ b\tau(1-\nu)+C^+_{n+1/2}+C^-_{n+1/2}\le1.\end{gathered}\tag{3.2}$$

Then difference relation (3.1) *is a TVD scheme.*

Proof. Rewriting (3.1) in the form

$$u_n^{k+1}=\left[u_n^k(1-b\tau(1-\nu))+C^+_{n+1/2}\Delta_{n+1/2}u^k-C^-_{n-1/2}\Delta_{n-1/2}u^k\right](1+\nu b\tau)^{-1}$$

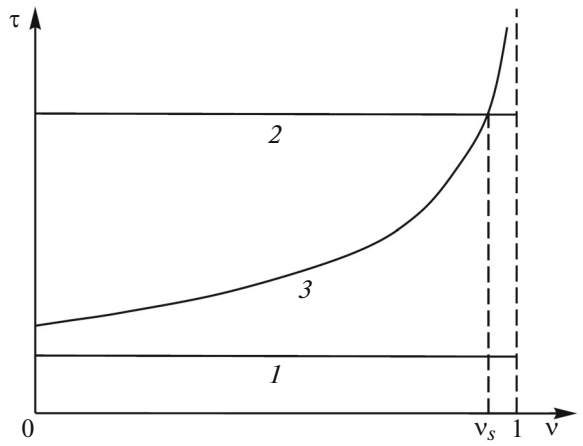

Fig. 1. Domains of an admissible time step as a function of the scheme parameter.

yields

$$\Delta_{n+1/2}u^{k+1} = \Big[\Big(1 - b\tau(1-\nu) - C^+_{n+1/2} - C^-_{n+1/2}\Big)\Delta_{n+1/2}u^k + C^+_{n+3/2}\Delta_{n+3/2}u^k + C^-_{n-1/2}\Delta_{n-1/2}u^k\Big](1+\nu b\tau)^{-1}.$$

Since all the coefficients are nonnegative, we have

$$\left|\Delta_{n+1/2}u^{k+1}\right| \le \Big[\Big(1 - b\tau(1-\nu) - C^+_{n+1/2} - C^-_{n+1/2}\Big)\left|\Delta_{n+1/2}u^k\right| + C^+_{n+3/2}\left|\Delta_{n+3/2}u^k\right| + C^-_{n-1/2}\left|\Delta_{n-1/2}u^k\right|\Big](1+\nu b\tau)^{-1}.$$

Summing this over $-\infty < n < +\infty$ gives

$$TV\left(u^{k+1}\right) = \sum_{n=-\infty}^{+\infty}\left|\Delta_{n+1/2}u^{k+1}\right| \le \Bigg[\sum_{n=-\infty}^{+\infty}\Big(1 - b\tau(1-\nu) - C^+_{n+1/2} - C^-_{n+1/2}\Big)\left|\Delta_{n+1/2}u^k\right| + \sum_{n=-\infty}^{+\infty}C^+_{n+3/2}\left|\Delta_{n+3/2}u^k\right| + \sum_{n=-\infty}^{+\infty}C^-_{n-1/2}\left|\Delta_{n-1/2}u^k\right|\Bigg](1+\nu b\tau)^{-1}$$

$$\le \sum_{n=-\infty}^{+\infty}\frac{1 - b\tau(1-\nu)}{1+\nu b\tau}\left|\Delta_{n+1/2}u^k\right| \le \sum_{n=-\infty}^{+\infty}\left|\Delta_{n+1/2}u^k\right| \le TV\left(u^k\right).$$

Inequality (3.2) can be rewritten as a time step constraint

$$\tau_T \le \frac{1 - C^+_{n+1/2} - C^-_{n+1/2}}{b(1-\nu)}, \quad \nu \ne 1. \tag{3.3}$$

For difference scheme (3.1) to be stable, it has to satisfy the Courant–Friedrichs–Lewy (CFL) condition

$$\tau_C \le \frac{h}{\max\limits_{\forall n} a(u)}. \tag{3.4}$$

Remark. In Fig. 1, the domains of admissible time steps determined by conditions (3.3) and (3.4) are shown as functions of the scheme parameter ν. The first case corresponds to a fine grid with $\tau_C \le \tau_T\ \forall\nu$. The time step is determined by CFL condition (3.4) (see Fig. 1, line *1*), and the sufficient TVD condition (line *3*) always holds. In the second case, $\tau_C > \tau_T$ for $\nu < \nu_s$. For example, the stiffness of the problem is exhibited when the cell size or the source intensity $b \gg 1$ is increased (Fig. 1, line *2*). As $\nu \to 1$, the time step determined by (3.3) can be arbitrarily large. It does not depend on the grid sizes or the source intensity

and is restricted by the stability condition (by the well-posedness of the difference problem [21]); i.e., scheme (3.1) is K-stable [14].

3.2. TVD Scheme for the Equations of Heterogeneous Wave Dynamics with Identical Phase Pressures

Consider a multiparameter family of difference schemes with parameters $\nu_1, \nu_2, \varepsilon_1, \varepsilon_2 \in [0, 1]$ and two-stage splitting. At the first stage (time level indexed by $k+1/2$), the convective terms are dropped. The difference relations are given for the one-dimensional case, since the scheme is easy to generalize to several dimensions. The quantities associated with $\mathbf{F}_\mu$ and Q are linearized about the point $\left(x_n, t^k\right)$ by applying a semi-implicit scheme [16] with coefficients b_v^k and b_T^k, respectively:

$$\rho_{1,n}^k \frac{v_{1,n}^{k+1/2} - v_{1,n}^k}{\tau} + \alpha_1^k \frac{\tilde{p}_{n+1/2}^k - \tilde{p}_{n-1/2}^k}{h} = -b_v^k \left(\nu_1 v_{1,n}^{k+1/2} + (1-\nu_1) v_{1,n}^k - \nu_2 v_{2,n}^{k+1/2} - (1-\nu_2) v_{2,n}^k\right),$$

$$\rho_{2,n}^k \frac{v_{2,n}^{k+1} - v_{2,n}^k}{\tau} + \alpha_2^k \frac{\tilde{p}_{n+1/2}^k - \tilde{p}_{n-1/2}^k}{h} = b_v^k \left(\nu_1 v_{1,n}^{k+1/2} + (1-\nu_1) v_{1,n}^k - \nu_2 v_{2,n}^{k+1/2} - (1-\nu_2) v_{2,n}^k\right),$$

$$\rho_{1,n}^k \frac{E_{1,n}^{k+1/2} - E_{1,n}^k}{\tau} + \rho_{2,n}^k \frac{\left(v_{2,n}^{k+1/2}\right)^2 - \left(v_{2,n}^k\right)^2}{2\tau} + \frac{\tilde{p}_{n+1/2}^k \left(\alpha_1^k v_1^k\right)_{n+1/2} - \tilde{p}_{n-1/2}^k \left(\alpha_1^k v_1^k\right)_{n-1/2}}{h}$$

$$= -b_T^k \left(\varepsilon_1 \left(E_{1,n}^{k+1/2} - \left(v_{1,n}^{k+1/2}\right)^2/2\right)/c_v + (1-\varepsilon_1)\left(E_{1,n}^k - \left(v_{1,n}^k\right)^2/2\right)/c_v \right. \tag{3.5}$$

$$\left. - \varepsilon_2 e_{2,n}^{k+1/2}/c_2 - (1-\varepsilon_2) e_{2,n}^k/c_2\right),$$

$$\rho_{2,n}^k \frac{e_{2,n}^{k+1/2} - e_{2,n}^k}{\tau} = b_T^k \left(\varepsilon_1 \left(E_{1,n}^{k+1/2} - \left(v_{1,n}^{k+1/2}\right)^2/2\right)/c_v \right.$$

$$\left. + \left((1-\varepsilon_1)\left(E_{1,n}^k - \left(v_{1,n}^k\right)^2/2\right)\right)/c_v - \varepsilon_2 e_{2,n}^{k+1/2}/c_2 - (1-\varepsilon_2) e_{2,n}^k/c_2\right), \quad \tilde{p}_{n\pm1/2}^k = p_{n\pm1/2}^k + q_{n\pm1/2}^k.$$

Here and below, the half-integer indices $n \pm 1/2$ denote cell boundaries and $q_{n\pm1/2}^k$ is the artificial viscosity.

Scheme (3.5) is represented in matrix form:

$$A_v \cdot U_v = B_v, \quad A_e \cdot U_e = B_e,, \tag{3.6}$$

where

$$U_v = \begin{pmatrix} v_{1,n}^{k+1/2} \\ v_{2,n}^{k+1/2} \end{pmatrix}, \quad A_v = \begin{pmatrix} \left(1 + \nu_1 b_v^k \tau/\rho_{1,n}^k\right), & -\nu_2 b_v^k \tau/\rho_{1,n}^k \\ -\nu_1 b_v^k \tau/\rho_{2,n}^k, & \left(1 + \nu_2 b_v^k \tau/\rho_{2,n}^k\right) \end{pmatrix},$$

$$B_v = \begin{pmatrix} v_{1,n}^k + \left[-\alpha_1^k \dfrac{p_{n+1/2}^k - p_{n-1/2}^k}{h} - b_v^k \left((1-\nu_1) v_{1,n}^k - (1-\nu_2) v_{2,n}^k\right)\right] \tau/\rho_{1,n}^k \\ v_{2,n}^k + \left[-\alpha_2^k \dfrac{p_{n+1/2}^k - p_{n-1/2}^k}{h} + b_v^k \left((1-\nu_1) v_{1,n}^k - (1-\nu_2) v_{2,n}^k\right)\right] \tau/\rho_{2,n}^k \end{pmatrix},$$

$$U_e = \begin{pmatrix} E_{1,n}^{k+1/2} \\ e_{2,n}^{k+1/2} \end{pmatrix}, \quad A_e = \begin{pmatrix} \left(1 + \varepsilon_1 b_T^k \tau/\rho_{1,n}^k/c_v\right), & -\varepsilon_2 b_T^k \tau/\rho_{1,n}^k/c_2 \\ -\varepsilon_1 b_T^k \tau/\rho_{2,n}^k/c_v, & \left(1 + \varepsilon_2 b_T^k \tau/\rho_{2,n}^k/c_2\right) \end{pmatrix},$$

$$B_e = \begin{pmatrix} B_{e1} \\ B_{e2} \end{pmatrix},$$

$$B_{e1} = E_{1,n}^k + \left(-\rho_{2,n}^k \left(\left(v_{2,n}^{k+1/2}\right)^2 - \left(v_{2,n}^k\right)^2\right)/2\tau - \left(\tilde{p}_{n+1/2}^k \left(\alpha_1^k v_1^k\right)_{n+1/2} - \tilde{p}_{n-1/2}^k \left(\alpha_1^k v_1^k\right)_{n-1/2}\right)\right.$$

$$\left. - b_T^k \left(\left(-\varepsilon_1 \left(v_{1,n}^{k+1/2}\right)^2/2 + (1-\varepsilon_1)\left(E_{1,n}^k - \left(v_{1,n}^k\right)^2/2\right)\right)/c_v - (1-\varepsilon_2) e_{2,n}^k/c_2\right)\right) \tau/\rho_{1,n}^k,$$

$$B_{e2} = e_{2,n}^k + b_T^k \left(\left(-\varepsilon_1 \left(v_{1,n}^{k+1/2} \right)^2 /2 + (1-\varepsilon_1) \left(E_{1,n}^k - \left(v_{1,n}^k \right)^2 /2 \right) \right) / c_v - (1-\varepsilon_2) e_{2,n}^k / c_2 \right) \tau / \rho_{2,n}^k,$$

$$E_{2,n}^{k+1/2} = e_{2,n}^{k+1/2} + \left(v_{2,n}^{k+1/2} \right)^2 /2.$$

At the first stage, the desired parameters are found explicitly by solving the systems of linear algebraic equations (3.6) with the help of Gaussian elimination.

The nonlinear artificial viscosity is determined by the formula

$$q_{n+1/2}^k = -\left[B\left(1 - \min\left(\max\left(0, r_v\right), 1\right)\right) + B_0 \min\left(\max\left(0, r_v\right), 1\right) \right] \times \sqrt{\gamma_1 p_{n+1/2}^k \left(\rho_{1,n+1/2}^k + D \rho_{2,n+1/2}^k \right)} \Delta_{n+1/2} v_1. \tag{3.7}$$

The parameter r_v is computed so as to satisfy the conditions

$$r_v = \begin{cases} \Delta_{n-1/2} v_1 / \Delta_{n+1/2} v_1 & \text{if} \quad \Delta_{n+1/2} p < 0 \quad \text{and} \quad \Delta_{n+1/2} v_1 < 0, \\ \Delta_{n+3/2} v_1 / \Delta_{n+1/2} v_1 & \text{otherwise.} \end{cases}$$

Here,

$$\Delta_{n+3/2} v_1 = v_{1,n+2}^k - v_{1,n+1}^k, \quad \Delta_{n+1/2} v_1 = v_{1,n+1}^k - v_{1,n}^k,$$

$$\Delta_{n-1/2} v_1 = v_{1,n}^k - v_{1,n-1}^k, \quad \Delta_{n-3/2} v_1 = v_{1,n-1}^k - v_{1,n-2}^k,$$

$$D = \begin{cases} 1 - \left(T^{(\mu)} / T_*^{(\mu)} \right) = 1 - \left(d/d_* \right)^2 & \text{if} \quad d \le d_*, \\ 0 & \text{otherwise,} \end{cases}$$

where $B, B_0 \ge 0$ are the artificial viscosity coefficients: nonlinear $B - B_0$ and linear B_0; $T^{(\mu)}$ and $T_*^{(\mu)}$ are the phase relaxation time and its characteristic value; and d and d_* are the diameter of the dispersed particles and its characteristic value.

The artificial viscosity (3.7) provides a nonlinear (adaptive) mechanism of smoothing the numerical solution. The transition from the second-order accurate difference scheme $O(h^2)$ on smooth solutions to the scheme with nonzero artificial viscosity of order $O(h)$ in regions of high gradients and extrema is performed depending on the slopes of the velocity projections at the first stage.

At the second stage, the convective terms of system (2.1) are approximated by upwind schemes with reconstruction of functions (see [9]):

$$\tilde{\varphi}_{i,n+1/2}^k = \begin{cases} \varphi_{i,n+1/2}^+, & v_{i,n+1/2}^{k+1/2} \ge 0, \\ \varphi_{i,n+1/2}^-, & v_{i,n+1/2}^{k+1/2} < 0, \end{cases} \quad \varphi = \{\rho_i, v_i, E_i, e_2\},$$

$$\varphi_{i,n+1/2}^+ = \left[\varphi_{i,n}^k + \frac{1}{2} \psi\left(r_{i,n+1/2}^+ \right) \left(1 - c_{i,n+1/2}\right) \left(\varphi_{i,n+1}^k - \varphi_{i,n}^k \right) \right],$$

$$\varphi_{i,n+1/2}^- = \left[\varphi_{i,n+1}^k - \frac{1}{2} \psi\left(r_{i,n+1/2}^- \right) \left(1 + c_{i,n+1/2}\right) \left(\varphi_{i,n+1}^k - \varphi_{i,n}^k \right) \right],$$

$$c_{i,n+1/2} = v_{i,n+1/2}^{k+1/2} \frac{\tau}{h}, \quad r_{i,n+1/2}^+ = \frac{\varphi_{i,n}^k - \varphi_{i,n-1}^k}{\varphi_{i,n+1}^k - \varphi_{i,n}^k}, \quad r_{i,n+1/2}^- = \frac{\varphi_{i,n+2}^k - \varphi_{i,n+1}^k}{\varphi_{i,n+1}^k - \varphi_{i,n}^k},$$

$$\psi(r) = \begin{cases} 0, & \text{Upwind}, \\ 1, & \text{Lax–Wendroff}, \\ \max\left[\min(2r,1), \min(r,2), 0\right], & \text{Superbee}, \\ (r + |r|)/(1+r), & \text{Van Leer}, \\ \min(r,1), & \text{MINMOD}, \\ \max\left[\min\left(2, 2r, \frac{1+r}{2}\right), 0 \right], & \text{MUSCL}, \end{cases} \tag{3.8}$$

$$\rho_i^{k+1} = \rho_i^k + \left(M_{i,n-1/2}^k - M_{i,n+1/2}^k\right)/h, \quad M_{i,n\pm1/2}^k = \tilde{\rho}_{i,n\pm1/2}^k v_{i,n\pm1/2}^{k+1/2}\tau,$$

$$\rho_{i,n}^{k+1} v_{i,n}^{k+1} = \rho_{i,n}^k v_{i,n}^{k+1/2} + \left(\tilde{v}_{i,n-1/2}^k M_{i,n-1/2}^{k+1/2} - \tilde{v}_{i,n+1/2}^k M_{i,n+1/2}^{k+1/2}\right)/h,$$

$$\rho_{2,n}^{k+1} e_{2,n}^{k+1} = \rho_{2,n}^k e_{2,n}^{k+1/2} + \left(\tilde{e}_{2,n-1/2}^k M_{2,n-1/2}^{k+1/2} - \tilde{e}_{2,n+1/2}^k M_{2,n+1/2}^{k+1/2}\right)/h,$$

$$E_{2,n}^{k+1} = e_{2,n}^{k+1} + \left(v_{2,n}^{k+1}\right)^2/2,$$

$$\rho_1^{k+1} E_1^{k+1} = \rho_1^k E_1^{k+1/2} - \left(\rho_2^{k+1} E_2^{k+1} - \rho_2^k E_2^{k+1/2}\right) + \sum_{i=1}^{2}\left(\tilde{E}_{i,n-1/2}^k M_{i,n-1/2}^{k+1/2} - \tilde{E}_{i,n+1/2}^k M_{i,n+1/2}^{k+1/2}\right)/h.$$

The time step is variable and is determined by the condition

$$\tau = \mathrm{CFL}\frac{h}{\max\limits_{\forall n}\left(\left|v_{1,n}^k\right| + a_{1,n}^k\right)},$$

where CFL is the Courant number and $a_{1,n}^k$ is the speed of sound in the gas at the point $\left(x_n, t^k\right)$.

4. NUMERICAL EXPERIMENTS

4.1. Test Problem

When the velocity and thermal relaxation times are small, a linear combination of Eqs. (2.1) yields the limiting equilibrium schemes

$$\frac{\partial\rho}{\partial t} + \nabla\cdot(\rho\mathbf{v}) = 0, \quad \frac{\partial\rho\mathbf{v}}{\partial t} + \nabla(\rho\mathbf{v}\mathbf{v}) + \nabla p = 0, \quad \frac{\partial\rho E}{\partial t} + \nabla\cdot(\rho E\mathbf{v}) + \nabla\cdot(p\mathbf{v}) = 0, \tag{4.1}$$

where $\mathbf{v} = \mathbf{v}_1 = \mathbf{v}_2$, $\rho = \rho_1 + \rho_2$, and $\rho E = \rho_1 E_1 + \rho_2 E_2$.

In the region of smooth flow, the energy equation of system (4.1) is equivalent to the quantity $S' = p\left((1 - C(x_2)\rho)/\rho\right)^\gamma$ preserved along the trajectories of mixture particles $dS'/dt = 0$ (see [22, 23]). The quantity $\gamma = \{\gamma_1, \gamma_2\}$ is equal to the ratio of specific heats γ_1 of the gas in the case of heat-insulated phases and to $\gamma_2 = \left(x_1 c_v + x_2 c_2 + x_1 R_1\right)/\left(x_1 c_v + x_2 c_2\right)$ in the case of thermal interphase equilibrium (see [1]), where R_1 is the gas constant and $x_i = \rho_i/\rho$ are the mass fractions of the phases. Taking into account that $dx_2/dt = 0$ along the trajectories of mixture particles, if the initial phase distribution is uniform, then $\gamma_2 \equiv \mathrm{const}$ and $C(x_2) = x_2/\rho_2^\circ \equiv \mathrm{const}$ do not vary with time $t \geq 0$.

As a test problem, we considered the initial stage of a two-phase flow from a plane channel of length L_1 with transverse size R_a to the axis of symmetry. The mixture consisted of an ideal gas (air, $\gamma_1 = 1.4$) and incompressible solid particles ($\rho_2^\circ = 2500$ kg/m^3). The origin was placed at the bottom of the channel on the axis of symmetry.

The initial conditions were specified as piecewise constant. Specifically, in the channel (for $0 \leq x \leq L_1$ and $0 \leq y \leq R_a$), we set uniformly distributed phase parameters $\mathbf{v}_i^{(1)} = 0$, $p^{(1)} = 10^6$ Pa, $T_i^{(1)} = 293$ K, and $\alpha_2^{(1)} = 0.01$; in the domain $L_2 \leq x < \infty$ and $0 \leq y < \infty$, there was a gas suspension with uniformly distributed phase parameters $\mathbf{v}_i^{(2)} = 0$, $p^{(2)} = 10^5$ Pa, $T_i^{(2)} = 293$ K, and $\alpha_2^{(2)} = 0.01$; and the parameters $\mathbf{v}_i^{(0)} = 0$, $p^{(0)} = 10^5$ Pa, $T_i^{(0)} = 293$ K, and $\alpha_2^{(0)} = 10^{-10}$ were specified in the rest of the domain, i.e., for $L_1 < x < L_2$ and $0 \leq y < \infty$. The particle sizes varied. Their values are given below. Impermeability conditions were set on the walls and the axis of symmetry, and "soft" boundary conditions of free flow were specified on the outer boundaries.

To compare numerical solutions produced by scheme (3.5)–(3.8) in the case when the observation time is much greater than the phase relaxation times, we used exact one-dimensional self-similar solutions of the Riemann and Hugoniot problems for an equilibrium two-phase medium (see [17, 22, 23]).

The Riemann invariants and the self-similar solution for rarefaction waves are given by

$$s = v - \frac{2}{\gamma-1}a\alpha_1, \quad r = v + \frac{2}{\gamma-1}a\alpha_1, \quad \alpha_1 = 1 - C(x_2)\rho,$$

$$\left(\frac{\alpha_{20}\alpha_1}{\alpha_2\alpha_{10}}\right)^{\omega} = \frac{\alpha_1+\omega}{\alpha_1(1\mp\omega\xi)}, \quad \frac{\mathrm{M}}{\alpha_{10}} = \left|\frac{2}{\gamma+2\alpha_1-1}(\alpha_1\xi\pm 1)\right|, \quad \frac{a\alpha_1}{a_0\alpha_{10}} = 1 - \frac{\omega}{\alpha_{10}}\mathrm{M}, \tag{4.2}$$

$$\frac{\rho\alpha_{10}}{\rho_0\alpha_1} = \left(1-\frac{\omega}{\alpha_{10}}\mathrm{M}\right)^{1/\omega}, \quad \frac{p}{p_0} = \left(1-\frac{\omega}{\alpha_{10}}\mathrm{M}\right)^{\gamma/\omega}, \quad \omega = \frac{\gamma-1}{2}, \quad \xi = \frac{x}{a_0\alpha_{10}t}, \quad \mathrm{M} = \frac{|v|}{a_0},$$

where M is the Mach number, $a = \sqrt{\gamma p/(\rho\alpha_1)}$ is the speed of sound in an equilibrium two-phase medium, and the index 0 denotes the initial parameter values.

The Hugoniot adiabat centered at (p_0, V_0, α_{10}) and the discontinuity relations for limiting schemes of interphase heat transfer have the form

$$\frac{p}{p_0} = \frac{\chi_0\alpha_2 - \alpha_{20}}{\chi\alpha_{20} - \alpha_2}, \quad \chi = \frac{\gamma+2\alpha_1-1}{\gamma-1}, \quad \chi_0 = \frac{\gamma+2\alpha_{10}-1}{\gamma-1},$$

$$\frac{V}{V_0} = \frac{\alpha_{20}}{\alpha_2}, \quad \frac{a^2}{a_0^2} = \frac{(\chi_0\alpha_2-\alpha_{20})\alpha_{20}\alpha_{10}}{(\chi\alpha_{20}-\alpha_2)\alpha_2\alpha_1}, \quad \frac{(v-v_0)^2}{a_0^2} = \mathrm{M}_0^2\left(\frac{\alpha_2-\alpha_{20}}{\alpha_2}\right)^2, \tag{4.3}$$

$$\mathrm{M}_0^2 = \frac{\alpha_{10}}{\gamma}\frac{(\chi_0+1)\alpha_2 - (\chi+1)\alpha_{20}}{\chi\alpha_{20}-\alpha_2}\frac{\alpha_2}{\alpha_2-\alpha_{20}}, \quad \mathrm{M}_0 = \frac{|v_0 - D_0|}{a_0}.$$

Here, $V = 1/\rho$ is the specific volume of the mixture and D_0 is the velocity of the shock wave.

The solution of the test problem in the one-dimensional flow region was constructed by matching simple waves (4.2) and (4.3), assuming that the velocity and pressure at the interface are continuous.

4.2. Numerical Results

Below are some numerical results obtained for the test problem described above. The parameters of the difference scheme were specified as $\nu_1 = \nu_2 = \varepsilon_1 = \varepsilon_2 = 1$, CFL = 0.5, $B = 1$, $B_0 = 0$, and $d_* = 1\ \mu\mathrm{m}$.

The one-dimensional computations were executed on a grid containing $N = 500$ cells with step $h = 0.001$ m at $L_1/Nh = 0.4$ and $L_2/Nh = 0.8$. In Fig. 2, the distributions of the relative velocity $v' = v/a^{(0)}$ and the relative density $\rho' = \rho/\rho^{(1)}$ along the axis $x' = x/Nh$ produced by scheme (3.5)–(3.8) with Superbee limiter (circles) at $d = 0.1\ \mu\mathrm{m}$ are compared with the exact self-similar limiting ($d \to 0$) solution in the case of thermal interphase equilibrium $\gamma = \gamma_2$ (4.2), (4.3) (solid line): (a) and (b) incident wave at $t_1 = 0.3$ ms; (e) and (f) shock waves transmitted and reflected from the gas mixture at $t_2 = 0.6$ ms.

The computed profiles of the relative particle velocity $v_2' = v_2/a^{(0)}$ at the corresponding times are shown by dotted curves. Figures 2c and 2d present the numerical results at $t_1 = 0.3$ ms obtained with various limiters: (*0*) Upwind; (*1*), (*2*) Superbee; (*3*) Van Leer; (*4*) Minmod; and (*5*) Muscl. The nonlinear artificial viscosity (3.7) with $B = 1$ and $B_0 = 0$ was used in all versions, except for scheme (*1*), where usual linear artificial viscosity ($B = 1$ and $B_0 = 1$) was applied. It can be seen that the computed shock wave profile is smeared to a substantially higher degree in the last case.

Figure 3 shows the two-dimensional results obtained at various times: (a), (b) $t_1 = 0.3$ ms; (c), (d) $t_2 = 0.5$ ms; and (e), (f) $t_3 = 0.7$ ms, namely, lines of equal relative gas density $\rho_1' = \rho_1/\rho_1^{(1)}$ depicted with a contour interval of 255 from 0.1001 to 0.999. The computations were conducted in a Cartesian coordinate system on a uniform grid with step $h = 0.001$ m and resolution $R_a/h = 200$ by applying the scheme with Superbee limiter, CFL = 0.4, $\nu_1 = \nu_2 = \varepsilon_1 = \varepsilon_2 = 1$, $B = 1$, $B_0 = 0.2$, and $d_* = 1\ \mu\mathrm{m}$. The geometric conditions of the problem were specified as $L_1/R_a = 2$ and $L_2/R_a = 4$. The numerical solutions were obtained for a dispersion medium with particle sizes $d = 0.1\ \mu\mathrm{m}$ (Figs. 3a, 3c, 3e) and $d = 50\ \mu\mathrm{m}$ (Figs. 3b, 3d, 3f).

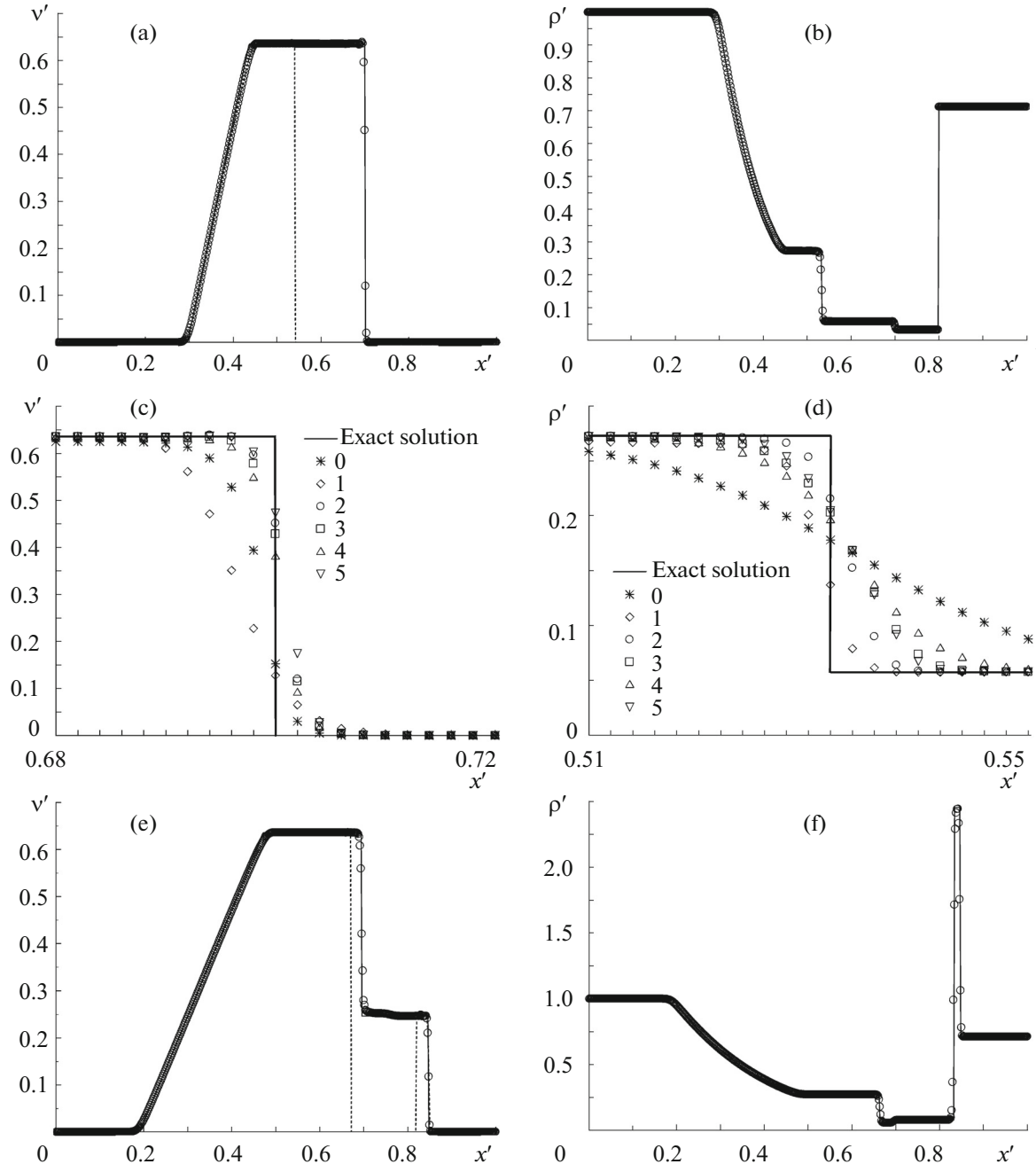

Fig. 2. Equilibrium flow ($d = 0.1$ μm): (a–d) incident wave, (e) and (f) the shock waves transmitted and reflected from the gas suspension.

Figure 3 shows some of the characteristic features of the heterogeneous flow detected in the computation: (*1*) the shock front after the decay of the initial discontinuity, (*2*) the contact discontinuity (jump in the gas density), (*3*) the rarefaction wavefront, (*4*) the front of the shock transmitted into the gas mixture, (*5*) combined discontinuity of the gas suspension (porosity discontinuity), (*6*) the front of the shock reflected from the gas suspension, (*7*) the contact discontinuity inside the gas suspension, (*8*) the front of the shock reflected from contact discontinuity (*2*), and (*9*) the transmitted shock front after the interaction of shock (*6*) with contact discontinuity (*2*). The dotted line marks the position of the combined discontinuity in the mixture flow; for fine particles ($d = 0.1$ μm), it nearly coincides with the contact discontinuity (Figs. 3a, 3c, 3e). In the case of nonequilibrium heterogeneous flow ($d = 50$ μm), the general

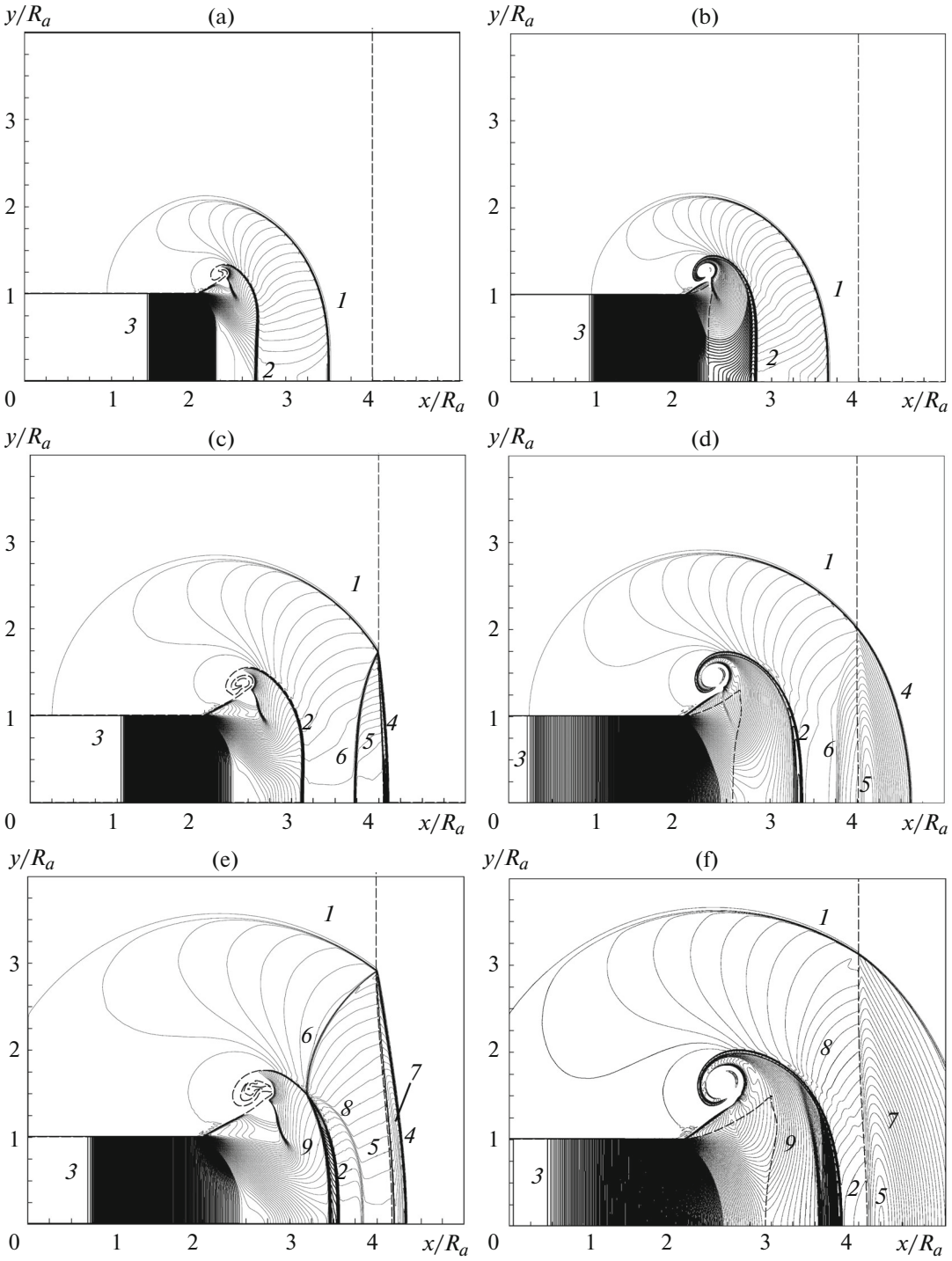

Fig. 3. Lines of equal relative gas density for (a), (c), (e) $d = 0.1$ μm and for (b), (d), (f) $d = 50$ μm.

flow pattern is preserved (see Figs. 3b, 3d, 3f). Due to the considerable slip of the phases, the initial shock splits into contact (*2*) and combined (dotted) discontinuities.

The computational efficiency of difference schemes was compared by applying the criterion from [24], which combines two properties: the accuracy of the numerical solution in some norm ε and the running time ET of the algorithm on the same computer:

$$CE^{-1} = \frac{\varepsilon_{\mathrm{I}} ET_{\mathrm{I}}}{\varepsilon_{\mathrm{II}} ET_{\mathrm{II}}}. \tag{4.4}$$

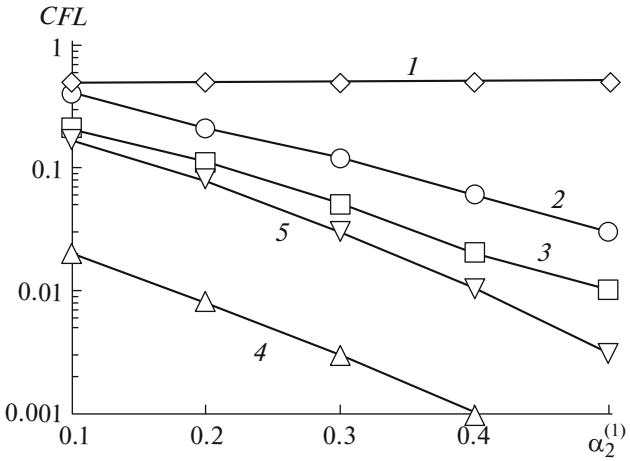

Fig. 4. Admissible Courant number vs. the volume particle fraction.

According to (4.4), scheme I is more efficient than scheme II if $CE > 1$.

Given a problem with a characteristic length L, suppose that the task is to determine the efficiency of scheme I against scheme II at the time T for given numerical accuracy $\varepsilon_I = \varepsilon_{II} \le \varepsilon$. Then criterion (4.4) can be represented in the form

$$CE^{-1} = \frac{\Delta t_I N_I^{\kappa+1} \mathrm{CFL}_I}{\Delta t_{II} N_{II}^{\kappa+1} \mathrm{CFL}_{II}}. \tag{4.5}$$

Here, Δt is the CPU time required for computing the parameters within a single grid cell in the transition to an upper time level; N is the number of cells along a single axis; and $\kappa = 1, 2,$ or 3 is the dimension of the problem.

Criterion (4.5) shows that, for $N_I = N_{II}$ and $\Delta t_I = \Delta t_{II}$, the computational efficiency of a difference scheme is determined by its stability margin (admissible Courant number CFL_*). We compare scheme I with $\nu_1 = \nu_2 = \varepsilon_1 = \varepsilon_2 = 1$ and scheme II with interphase interactions taken into account at the lower time level ($\nu_1 = \nu_2 = \varepsilon_1 = \varepsilon_2 = 0$). Figure 4 displays CFL_* as a function of the volume particle fraction $\alpha_2^{(1)}$ for various cell sizes and particle diameters as obtained in the numerical solution of the one-dimensional test problem. The computations confirm that the stability margin of scheme I is independent of the volume particle concentration, the spatial mesh size, or the particle sizes (line *1*). In the case of scheme II, CFL_* is reduced with increasing $\alpha_2^{(1)}$ and decreasing particle diameter: (*2*) $d = 10$ μm, (*3*) $d = 5$ μm, and (*4*) $d = 1$ μm for $h = 0.01$ m; additionally, it depends on the cell size: (*5*) $d = 1$ μm for $h = 0.001$ m.

Let us estimate the efficiency of the proposed scheme, for example, with Superbee limiter as compared with the first-order Upwind scheme in (3.8) for various problem dimensions κ in the case of identical parameters $\nu_1 = \nu_2 = \varepsilon_1 = \varepsilon_2 = 1$ and the Courant number CFL. To achieve the prescribed (identical for both schemes) resolution for the contact discontinuity (see Fig. 2d), Upwind must be implemented on a grid that is finer by more than five times; therefore, $N_1/N_2 \approx 1/5$. At the same time, the scheme with Superbee limiter requires roughly five times more CPU time for the computation in a single grid cell in the transition to an upper time level. Accordingly, the estimated efficiency of the difference scheme as applied to the one-, two-, and three-dimensional problems is 5, 25, and 125, respectively.

5. CONCLUSIONS

The difference scheme represented is applicable to heterogeneous flow problems with dominated convection (of hyperbolic or nonhyperbolic type). The stability of the scheme is independent of the grid size or the interphase interaction intensity, which can be useful in multidimensional computations or, for example, when it not known beforehand about the formation of solution singularities (discontinuities) or stiffness manifestation.

REFERENCES

1. R. I. Nigmatulin, *Fundamentals of Mechanics of Heterogeneous Media* (Nauka, Moscow, 1987).
2. M. Baer and J. Nunziato, "A two-phase mixture theory for the deflagration-to detonation transition (DDT) in reactive granular materials," Int. J. Multiphase Flows **12**, 861–889 (1986).
3. R. Saurel and R. Abgrall, "A multiphase Godunov method for compressible multifluid and multiphase flows," J. Comput. Phys. **150** (2), 425–467 (1999).
4. A. A. Zhilin and A. V. Fedorov, "Applying the TVD scheme to calculate two-phase flows with different velocities and pressures of the components," Math. Models Comput. Simul. **1** (1), 72–87 (2008).
5. D. V. Sadin, V. O. Guzenkov, and S. D. Lyubarskii, "Numerical study of the structure of a finely disperse unsteady two-phase jet," J. Appl. Mech. Tech. Phys. **46** (2), 224–229 (2005).
6. F. Petitpas, E. Franquet, R. Saurel, and O. Le Metayer, "A relaxation-projection method for compressible flows: Part II. Artificial heat exchanges for multiphase shocks," J. Comput. Phys. **225** (2), 2214–2248 (2007).
7. R. Saurel, F. Petitpas, and R. A. Berry, "Simple and efficient relaxation methods for interfaces separating compressible fluids, cavitating flows and shocks in multiphase mixtures," J. Comput. Phys. **228** (5), 1678–1712 (2009).
8. O.-B. Fringer, S. W. Armfield, and R. L. Street, "Reducing numerical diffusion in interfacial gravity wave simulations," Int. J. Numer. Methods Fluids **49**, 301–329 (2005).
9. C. Hirsch, *Numerical Computation of Internal and External Flows*, Vol. 2: *Computational Methods for Inviscid and Viscous Flows* (Wiley, New York, 1990)
10. D. A. Tropin and A. V. Fedorov, "High-order accurate numerical scheme for simulating the dynamics of a mixture of reactive gases and inert particles," Vychisl. Tekhnol. **18** (4), 64–76 (2013).
11. G. Chen, C. Levermore, and T. Liu, "Hyperbolic conservation laws with stiff relaxation terms and entropy," Commun. Pure. Appl. Math. **47**, 787–830 (1994).
12. D. V. Sadin, "A modified large-particle method for calculating unsteady gas flows in a porous medium," Comput. Math. Math. Phys. **36** (10), 1453–1458 (1996).
13. D. V. Sadin, "Stiffness problem in modeling wave flows of heterogeneous media with a three-temperature scheme of interphase heat and mass transfer," J. Appl. Mech. Tech. Phys. **43** (2), 286–290 (2002).
14. D. V. Sadin, "On stiff systems of partial differential equations for motion of heterogeneous media," Mat. Model. **14** (11), 43–53 (2002).
15. A. A. Gubaidullin, A. I. Ivandaev, and R. I. Nigmatulin, "A modified "coarse particle" method for calculating nonstationary wave processes in multiphase dispersive media," Comput. Math. Math. Phys. USSR **17** (6), 180–192 (1977).
16. D. V. Sadin, "A method for computing heterogeneous wave flows with intense phase interaction," Comput. Math. Math. Phys. **38** (6), 987–993 (1998).
17. D. V. Sadin, "Stiff problems of a two-phase flow with a complex wave structure," Fiz.-Khim. Kinetika Gaz. Din. **15** (4), 1–17 (2014).
18. L. E. Sternin, B. P. Maslov, A. A. Shraiber, and A. M. Podvysotskii, *Two-Phase Mono- and Polydispersed Gas-Particle Flows* (Mashinostroenie, Moscow, 1980) [in Russian].
19. A. F. Chudnovskii, *Heat Transfer in Dispersions* (Gostekhteorizdat, Moscow, 1954) [in Russian].
20. A. Harten, "High resolution schemes for hyperbolic conservation laws," J. Comput. Phys. **49**, 357–393 (1983).
21. D. V. Sadin, "On the convergence of a certain class of difference schemes for the equations of unsteady gas motion in a disperse medium," Comput. Math. Math. Phys. **38** (9), 1508–1513 (1998).
22. A. S. Ivanov, V. V. Kozlov, and D. V. Sadin, "Unsteady flow of a two-phase disperse medium from a cylindrical channel of finite dimensions into the atmosphere," Fluid Dyn. **31** (3), 386–391 (1996).
23. D. V. Sadin, *Fundamentals of the Theory of Modeling Wave Heterogeneous Processes* (Voennyi Inzh.-Kosmich. Univ., St. Petersburg, 2000) [in Russian].
24. C. A. J. Fletcher, *Computational Techniques for Fluid Dynamics* (Springer-Verlag, Berlin, 1990; Mir, Moscow, 1991), Vol. 1.

Translated by I. Ruzanova